Research on Recognition and Estimation Algorithm for Real time Changes in the Center of Gravity of Human Sitting Quality

Jingbin Yang[1], Xiumin Shi[2, *], Yuming Qi[2], and Sanpeng Deng[2]

[1] Institute of Robotics and Intelligent Equipment, Tianjin University of Technology and Education, Tianjin 300222, China

[2] Tianjin Key Laboratory of Intelligent Robot Technology and Application, Tianjin 300350, China

Abstract

This article explores the interference estimation problem of human body mass changes and shaking in the sitting posture of medical transport nursing robots in medical scenarios. Due to the significant time-varying and uncertain load characteristics caused by patients' vital signs and behaviors, including strong randomness and non-linearity, high requirements are placed on the speed tracking accuracy and anti-interference ability of the robots. When developing high-performance decision-making and control algorithms for transport robots, the estimation of the mass of the seated human body and the shaking angle are basic parameters that must be considered. Due to the fact that the shaking of the seated human body can cause changes in the mass of the seated human body, there is a tight coupling problem, and the existing recognition algorithms for the shaking angle of the seated human body have insufficient adaptability to working conditions, which affects the accuracy and convergence speed of the estimation algorithm. However, existing research on incomplete wheeled robots mainly focuses on the analysis methods represented by Newton vector mechanics systems and Lagrange equations. However, there are still shortcomings in analyzing the uncertainty of the robot's internal dynamics model and external disturbances, especially in dealing with parameter mismatch and nonlinear oscillation problems. To address this issue, this paper proposes a dynamic modeling method based on the Lagrangian equation of the dissipation function. By incorporating threshold switching to improve the adaptive recursive least squares method and combining it with the adaptive unscented Kalman filtering algorithm, real-time adaptive estimation of human sitting posture mass and difficult to measure human body sway pitch angle is performed using drive wheel torque data. Through comparison between the pre - and post improvement algorithms, the improved estimation algorithm improves speed and accuracy.

Keywords

Medical Transfer Nursing Robot; Human Sitting Posture; Parameter Estimation; Adaptive Unscented Kalman Filter.

1. Introduction

With the rapid development of intelligent manufacturing and logistics automation technology, the application of transport robots in warehousing logistics, flexible production lines and other scenarios is becoming increasingly widespread[1]. In actual operation, transport robots often need to handle objects of different masses and volumes (such as irregular packages, components, etc.), resulting in significant time-varying and uncertain load characteristics. In the field of smart healthcare, medical transportation and nursing robots are gradually replacing traditional manual transportation methods and becoming the core equipment for patient transportation in hospitals.[2] Unlike industrial scenarios, robots in medical transportation carry patients with vital signs, and their modeling has three special characteristics: (1) strong randomness of load: patient sitting posture adjustment, limb movement (such as coughing, sneezing, etc.), etc. can cause random changes in the load mass of the transportation robot; (2) Strong nonlinearity of load: Changes in the mass of the load and the shaking of the patient can disrupt the superposition of the robot's linear system. For example, when the patient rapidly shakes their body, the centrifugal force generated is proportional to the square of the angular velocity and has quadratic nonlinearity. (3) Strict safety restrictions: The hospital environment is complex, and any dynamic instability may cause secondary injuries. This requires the robot to maintain millimeter level trajectory accuracy and anti-interference ability under variable load conditions.

With the continuous development of estimation theory, researchers are increasingly focusing on using existing robot sensors to obtain partial robot state information, and fusing these sensor data through kinematic or dynamic methods to estimate state parameters that are difficult to measure directly. At present, the estimation methods for human body mass and body sway in sitting posture are mainly based on dynamic models and sensor data fusion methods. It relies on the precise establishment of the model and the calculation of the controller, taking into account coupling effects such as vehicle speed, acceleration, torque, sitting posture and human body shaking. However, due to the close coupling relationship between the mass of the sitting human body and the shaking of the sitting human body on the tires, a distributed modular strategy is usually used for estimation [3]. For example, Li[4] et al. proposed a two-step estimator combined with a dynamical model. Hu[5] et al. used the recursive least squares method with adaptive forgetting factor and the extended Kalman filter algorithm for quality estimation. Mattila[6] et al. proposed a method to judge the motion stability of mobile manipulators by combining the stability domain and pressure sensor data. Wang[7] et al. proposed a sensor-based mass estimation algorithm, and established methods for road slope compensation and mass estimation error compensation. Cai[8] et al. used the recursive least square method to estimate the road slope based on sensor data, and used it as the algorithm observation to estimate the quality of the extended Kalman filter algorithm. Chen[9] et al. used the Kalman filter theory to propose an estimator with two-step measurement update to estimate the yaw Angle and roll Angle through the acceleration and angular velocity signals of the IMU sensor.However, the traditional Kalman filter is mainly suitable for linear systems. For systems with nonlinear characteristics, the use of the classical Kalman filter method will be limited. In order to deal with this challenge, the extended Kalman filter came into being, Li[10] et al. linearized the system by the Jacobian matrix, so as to be suitable for the state estimation of nonlinear systems. He[11] et al. designed unscented Kalman filter (UKF) to estimate vehicle parameters in real time. The probability distribution of the original system is represented by a set of Sigma points, which can preserve the mean and covariance of the original system, so as to avoid the error accumulation problem caused by the linearization of high-order small terms in Taylor expansion. Zhang[12] et al. proposed an estimation method based on enhanced adaptive Unscented Kalman filter for vehicle state estimation under unknown noise conditions.

There are two typical problems in the existing systems, especially when transferring patients with mobility and sudden convulsions or emergency obstacle avoidance: (1) Parameter mismatch: the inertia change exceeds 200% due to the weight difference of patients (50-100kg for adults), and the fixed parameter PID control overtakes; (2) Nonlinear oscillation: the flexible shaking of the human body and the driving wheel cause low-frequency flutter. We refer to the above problem as the variable load problem. Since the UKF avoids the complexity of the linearization step and the possible inaccuracy introduced, it is able to provide more precise and reliable state estimates when dealing with complex nonlinear systems. This advantage enables it to provide more accurate state information for speed tracking control of medical transport care robots, thus ensuring the stability and safety of the control system under various driving conditions. Aiming at the above problems, this paper proposes a dynamic modeling and variable load state estimation method considering sitting human

ISSN: 2414-1895 DOI: 10.6919/ICJE.202510_11(10).0017

body. The dynamic model of robot considering variable load is established based on the Lagrange equation of dissipation function. The variable load disturbance and unmodeled disturbance are estimated and compensated online by driving wheel sensor data and state observer, so that the state information fed back to the controller is more rapid, smooth and close to the true value.

2. Overall Structure of Medical Transport Nursing Robot

2.1 Whole Machine Structure

The structure of the medical transport nursing robot includes an open-and-close rotating seat, a lifting electric push rod, a front and rear laser radar, two servo driving wheels in front, and two driving wheels in back. The robot body adopts a differential drive mode, and the open-and-close rotating seat for the patient is located above the transport robot, as shown in Figure 1.

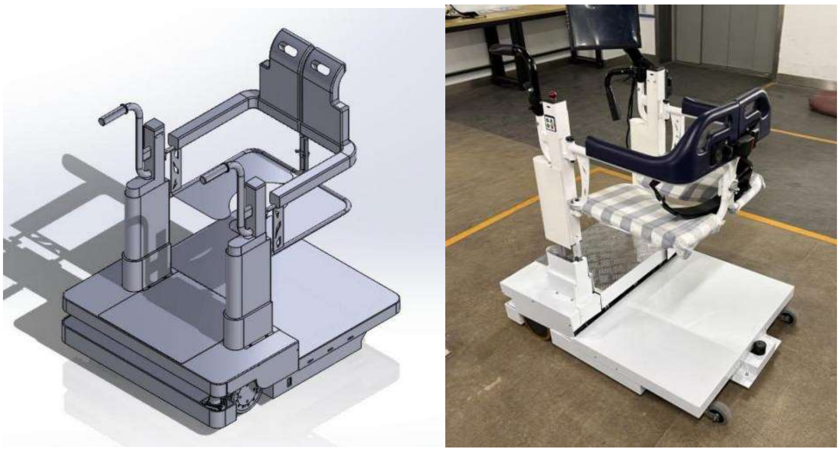

Figure 1. Model of medical transport care robot

Table 1. Medical transport nursing machine system variable table

System variable definition	Symbol
Robot quality(kg)	m
Sitting body mass(kg)	m_h
Drive wheel radius(m)	r
wheel spacing(m)	L
Robot angular velocity(*rad/s*)	$\omega, \dot{\theta}$
Robot speed(*m/s*)	v
Left/right wheel linear speed(*m/s*)	v_l / v_r
Left/right wheel drive torque(*Nm*)	τ_l / τ_r
Left/right wheel angular velocity(*rad/s*)	φ_l / φ_r
The length of the upper body of the human body(*m*)	h
Pitch Angle of the human body(*rad*)	φ_x
Tilt Angle of the human body(*rad*)	φ_y
The moment of inertia of the human body(*kg m*^{2})	I_h
The steering torque of the robot's center of mass(*Nm*)	τ_c

The variable load of medical transfer care robots includes two situations. One is that the mass of the robot load changes, and the patient and his items are the loads of the robot. With the difference of no-load, on-load and the weight of the patient and his items, the overall mass of the robot load will also be different. The other is that the robot load is randomly sloshing.

In order to clearly define the robot parameter variables, the variable table of medical transport nursing machine system as shown in Table 1 is constructed.

2.2 Kinematic Model of Medical Transport Care Robot

The medical transfer care robot is composed of a chassis structure with two servo-driven wheels at the front and two swivel wheels at the back. The world coordinate system satisfies the right-hand rule as $\{O, X_I, Y_I, Z_I\}\}$. In the robot's own coordinate system, the center of the robot's shape is defined as the origin of the coordinate system, its forward direction is the X-axis, the left side of the robot is the Y-axis, following the right-hand rule, and the direction perpendicular to the robot's plane is the Z-axis, thus obtaining the robot's coordinate system as $\{C, X_R, Y_R, Z_R\}$. The kinematic model of the medical transfer care robot is shown in Figure 2.

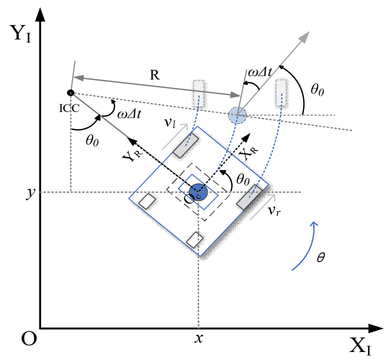

Figure 2. Histogram equalization

In the world coordinate system,it is denoted as (x,y,θ), where x and y denote the coordinates of the robot center in the world coordinate system.θ represents the robot heading Angle,Its value is the Angle between the X-axis of the local coordinate system and the X-axis of the global coordinate system,The initial heading Angle can be set to θ_0, and when the robot turns, its steering heading angular velocity is ω, which is positive counterclockwise.

The generalized coordinate vector ξ_I, the local coordinate vector ξ_R, and the orthogonal rotation matrix between the global coordinate system and the local coordinate system is $R(\theta)$

$$\xi_I=\begin{bmatrix} x_I \\ y_I \\ \theta \end{bmatrix},\ \xi_R=\begin{bmatrix} x_R \\ y_R \\ \theta \end{bmatrix},\ \xi_R=R(\theta)\xi_I,\ \boldsymbol{R}(\theta)=\begin{bmatrix} \cos\theta & \sin\theta & 0 \\ -\sin\theta & \cos\theta & 0 \\ 0 & 0 & 1 \end{bmatrix} \tag{1}$$

Among them, ξ_I is the generalized coordinate vector, ξ_R is the local coordinate vector, $R(\theta)$ is the orthogonal rotation matrix between the global coordinate system and the local coordinate system, x and y are the global coordinate positions, x_c and y_c are the positions of the robot coordinate system, and θ is the robot heading angle.

The differential robot is a non-holonomic constrained mobile robot. The non-slip motion of the robot perpendicular to the forward direction is expressed in the following equation

$$\dot{x}\sin\theta - \dot{y}\cos\theta = 0 \tag{2}$$

ISSN: 2414-1895 DOI: 10.6919/ICJE.202510_11(10).0017

Where $\dot{x},\dot{y}$ is the velocity along the X-axis and Y-axis of the global coordinate system, and θ is the heading Angle of the robot.

The linear velocity direction of the driving wheel is related to the linear velocity direction of the robot as follows

$$\dot{x}_c=\frac{(\dot{\varphi}_r+\dot{\varphi}_l)r}{2},\dot{y}_c=0,\dot{\theta}=\frac{(\dot{\varphi}_r-\dot{\varphi}_l)r}{L} \tag{3}$$

where $\dot{\varphi}_l$ and $\dot{\varphi}_r$ represent the angular velocities of the left and right driving wheels respectively, r is the radius of the driving wheel, and L is the distance between the left and right driving wheels.

The expression for the left and right driving wheels doing pure rolling motion is as follows

$$\begin{cases}\dot{x}\cos\theta+\dot{y}\sin\theta+L\dot{\theta}-\dot{r}\varphi_1=0\\ \dot{x}\cos\theta+\dot{y}\sin\theta-L\dot{\theta}-\dot{r}\varphi_1=0\end{cases} \tag{4}$$

Integrating the above equation), the forward kinematics model of the medical transport nursing robot in the global coordinate system with the speed control quantities and as input quantities can be obtained as follows

$$\dot{\boldsymbol{\xi}}_I=\boldsymbol{R}(\theta)^{-1}\dot{\boldsymbol{\xi}}_R=\begin{bmatrix}\dot{x}\\ \dot{y}\\ \dot{\theta}\end{bmatrix}=\begin{bmatrix}cos\,\theta & 0\\ sin\,\theta & 0\\ 0 & 1\end{bmatrix}\begin{bmatrix}v\\ \omega\end{bmatrix}=\boldsymbol{SV} \tag{5}$$

where $\boldsymbol{S}$ is the coordinate transformation matrix, $\boldsymbol{V}$ represents the velocity matrix.

The forward kinematic model of a medical transportation and care robot that uses speed as the control input quantity can be expressed as

$$\dot{\boldsymbol{\xi}}_I=\boldsymbol{R}(\theta)^{-1}\dot{\boldsymbol{\xi}}_R=\boldsymbol{R}(\theta)^{-1}\begin{bmatrix}\frac{r\dot{\varphi}_r}{2}+\frac{r\dot{\varphi}_l}{2}\\ 0\\ \frac{r\dot{\varphi}_r}{L}+\frac{-r\dot{\varphi}_l}{L}\end{bmatrix}=\begin{bmatrix}\frac{r\cos\theta}{2} & \frac{r\cos\theta}{2}\\ \frac{r\sin\theta}{2} & \frac{r\sin\theta}{2}\\ \frac{r}{L} & -\frac{r}{L}\end{bmatrix}\begin{bmatrix}\dot{\varphi}_r\\ \dot{\varphi}_l\end{bmatrix}=\boldsymbol{P}\dot{\boldsymbol{\varphi}} \tag{6}$$

where $\boldsymbol{P}$ is the driving wheel angular velocity input transformation matrix, $\dot{\boldsymbol{\varphi}}$ represents the matrix of the angular velocity of the driving wheel

$$\begin{bmatrix}\dot{\varphi}_l\\ \dot{\varphi}_r\end{bmatrix}=\begin{bmatrix}\frac{2}{r\sin\theta} & -\frac{1}{r\cos\theta} & \frac{L}{4r}\\ \frac{2}{r\sin\theta} & -\frac{1}{r\cos\theta} & -\frac{L}{4r}\end{bmatrix}\dot{\xi}_I \tag{7}$$

During the transfer operation, the inertial force generated by the swaying of a seated human body can disrupt the robot's linear system, posing higher requirements for speed tracking control. It is necessary to establish a robot dynamics model considering a seated human body to compensate for the impact of variable load disturbances on the robot's speed tracking.

ISSN: 2414-1895 DOI: 10.6919/ICJE.202510_11(10).0017

2.3 Human Dynamics Analysis in Sitting posture

The two-degree-of-freedom model of the sitting human body is not coupled laterally with vertically [13]. Therefore, the human dynamic model reflecting the transverse-longitudinal direction only needs to satisfy the human dynamic characteristics under uniaxial excitation and reasonably design the topology. Medical transport nursing robot adopts non-slip cushion and backrest, at low speed operation, the interface between human and chair does not slip, that is, the robot's lateral and longitudinal motion input is directly transmitted to the human upper body, considering its body coordination ability is generally weak, the armrest and backrest may not be fully utilized when riding, so the armrest and backrest model is adopted. The influence of the sitting human body on the robot motion is amplified, and the coupled dynamics model is established. The longitudinal sitting human model and the lateral sitting human model are shown in Figures 3 and 4.

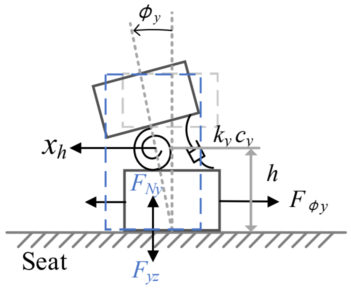

Figure 3. Longitudinal sitting mannequins

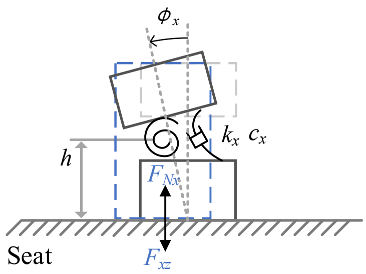

Figure 4. Lateral sitting mannequin

The mechanism of human body dynamics in sitting posture is analyzed, which is divided into longitudinal and transverse models. Pitch Angle is used for the longitudinal rocking Angle φ_y,Use the roll Angle for the left and right shaking Angle φ_x,The body rocking back and forth in the sitting posture will directly affect the load resistance moment of the driving wheel of the medical transfer nursing robot and the sum of the mixed resistance of the left and right driving wheels, and affect the speed stability of the left and right driving wheels.

The transverse and longitudinal sitting human body consists of spring damping and two mass blocks. When calculating, the upper body of the sitting human body is regarded as a homogeneous rod, and the transverse and longitudinal elastic potential energy of the sitting human body is obtained V_{mk}, According to the energy dissipation principle [14], the dissipation function can be obtained D

$$\begin{cases} V_{mk} = \frac{1}{2}k_x{\varphi_x}^2 + \frac{1}{2}k_y{\varphi_y}^2 \\ D = \frac{1}{2}c_y\dot{\varphi}_y^2 + \frac{1}{2}c_x\dot{\varphi}_x^2 \end{cases} \tag{8}$$

where k_x and $c_x$are the stiffness and damping values of the upper body and lower body of the longitudinal sitting human body, k_y and c_y are the stiffness and damping values of the upper body and lower body of the transverse sitting human body.

The human body coordinate system $\{H, X_m, Y_m, Z_m\}$ is established, and the human body horizontal and vertical coordinate system coincides with the robot coordinate system, which conforms to the right-hand rule.

Assuming that the vertical distance from the center of mass of the sitting human body to the center of mass of the seat is h, and the height of the car seat is h_c, the height of the center of mass of the

ISSN: 2414-1895 DOI: 10.6919/ICJE.202510_11(10).0017

sitting human body is $h_m=h_c+h$, and the position of the center of mass of the sitting human body in the robot coordinate system can be expressed as

$$\boldsymbol{r}_{\mathrm{h}0}=\begin{bmatrix}0\\0\\\mathrm{h}_m\end{bmatrix} \tag{9}$$

where h_m represents the height of a person's sitting position.

Given the coordinates of the center of mass of the car, the pitch Angle, roll Angle and height of the sitting human body, the position of the human body center in the world coordinate system can be obtained as follows

$$\boldsymbol{r}_{\mathrm{h}}=\begin{bmatrix}x+h(\cos\theta\sin\varphi_y\cos\varphi_x+\sin\theta\sin\varphi_x)\\y+h(\sin\theta\sin\varphi_y\cos\varphi_x-\cos\theta\sin\varphi_x)\\h_c+h\cos\varphi_y\cos\varphi_x\end{bmatrix} \tag{10}$$

where x and y represent the position of the robot, θ represents the heading angle of the robot, φ_x represents the lateral tilt angle of the human sitting posture, and φ_y represents the pitch angle of the human sitting posture.

Considering that the slog torque generated by the lateral leaning of the sitting human body has no direct effect on the driving force of the robot, only the position of the robot's center of mass and the rolling resistance of the driving wheel are changed, and the linear velocity of the human body's center of mass is simplified after ignoring the high-order small quantity and the roll Angle

$$\boldsymbol{v}_{\mathrm{h}}=\dot{r}_{\mathrm{h}}\approx\begin{bmatrix}\dot{x}+\mathrm{h}\left(-\sin\theta\,\dot{\theta}\varphi_y+\cos\theta\,\dot{\varphi}_y\right)\\\dot{y}+\mathrm{h}\left(\cos\theta\,\dot{\theta}\varphi_y+\sin\theta\,\dot{\varphi}_y\right)\\\mathrm{h}\left(-\varphi_y\dot{\varphi}_y\right)\end{bmatrix} \tag{11}$$

where $\dot{x}$ represents the speed in the X-axis direction of the robot's world coordinate system, $\dot{y}$ represents the speed in the Y-axis direction of the robot's world coordinate system, $\dot{\theta}$ represents the heading angle speed of the robot's world coordinate system, and $\dot{\varphi}_y$ represents the pitch angle speed of the human body's sitting posture.

Expression of human kinetic energy

$$T_m=\frac{1}{2}m_h\|\boldsymbol{v}_{\mathrm{h}}\|^2+\frac{1}{2}I_{\mathrm{h}}\left(\dot{\varphi}_x^2+\dot{\varphi}_y^2\right) \tag{12}$$

where m_h represents the body weight in a sitting position, and v_{h} represents the speed of the body in a sitting position.

Human body potential energy expression

$$V_m=m_h\mathrm{g}\mathrm{h}\cos\varphi_x\cos\varphi_y+\frac{1}{2}k_x{\varphi_x}^2+\frac{1}{2}k_y{\varphi_y}^2 \tag{13}$$

Volume 11 Issue 10, 2025
DOI: 10.6919/ICJE.202510_11(10).0017

where φ_x represents the lateral inclination angle of the human body in a sitting position, φ_y represents the pitch angle of the human body in a sitting position, k_x represents the coefficient of the lateral spring, and k_y represents the coefficient of the pitch spring, g represents the acceleration due to gravity.

2.4 Dynamic Model of Medical Transport Nursing Robot Considering Variable Load

The motion of the driving wheel relative to the ground is a composite motion of forward rolling and lateral sliding. The active torque of the driving wheel edge acting on the ground is T, and the force of the ground acting on the wheel can be decomposed into the forward tire rolling force F_w. When the wheel is affected by the driving torque (T>0), that is, clockwise direction, the driving force direction is forward (F_w>0), which is the driving force of the wheel. When the wheel is subjected to the braking torque (T<0), that is, the counterclockwise direction and the driving force direction is backward (F_w<0), which is the braking force of the wheel. The expression of the force and torque acting on the wheel is

$$\begin{cases} m_w\ddot{X}_c = F_W - X \\ I_0\dot{\varphi} = T - rF_W \end{cases} \tag{14}$$

where m_w represents the tire quality, $\ddot{X}_c$ represents the acceleration of the robot's forward movement, F_w represents the driving force, X represents the rolling resistance, I_0 represents the rotational inertia of the driving wheel, $\dot{\varphi}$ represents the angular velocity of the driving wheel, T represents the motor driving torque, and r represents the radius of the driving wheel.

The above formula always holds when the driving wheel is accelerating or slowing down.

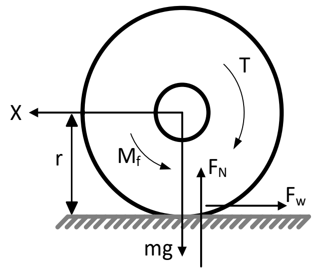

Figure 5. Force and torque analysis of driving wheel

The reason of rolling obstacle moment is as follows: when the wheel rolls forward, the ground supporting reaction point moves forward a deviation distance due to the deformation at the contact point between the wheel and the ground, then the ground supporting reaction force F_N produces an obstacle moment M_f relative to the wheel center, that is, rolling obstacle moment. As long as the wheel is moving forward, regardless of the acceleration rotation or deceleration rotation, the direction of the rolling obstacle torque is counterclockwise as shown in the figure, which always plays the role of hindering the wheel rotation. The rolling resistance F_f can be expressed as follows

$$F_f = \frac{M_f}{r} \tag{15}$$

where M_f represents the obstructive moment, r represents the radius of the driving wheel.

ISSN: 2414-1895 DOI: 10.6919/ICJE.202510_11(10).0017

The robot design process considers the force distribution of the chassis tire, that is, the weight of the robot body is evenly distributed on the four wheels, then the sitting posture of the human body of each wheel is

$$Z=\frac{1}{4}mg \tag{16}$$

where m represents the mass of the robot.

The force analysis of the wheel shows that the wheel is subjected to the downward body of the vertical ground plus its own gravity and the upward ground support force of the vertical ground. The wheel mass is 1/100 of the body mass, so the ground support force to each wheel is

$$F_N=Z+m_w g=\frac{13}{50}mg \tag{17}$$

Engineering tests show that the coefficient of rolling resistance is defined as the ratio of rolling resistance to the ground support reaction force

$$f=\frac{F_f}{F_N} \tag{18}$$

Among them, F_f represents rolling resistance and F_N represents the ground reaction force.

The rolling resistance coefficients f between different materials have been measured through engineering experiments and their range of values has been determined.

The rolling obstacle force of the driving wheel on each side is the sum of the rolling obstacle force of one driving wheel and one universal wheel on one side. Here, the sum of the rolling obstacle force of two driving wheels and twenty universal wheels of the robot is set as

$$F_f=F_{fr}+F_{fl}=2f_r F_N+2f_l F_N=\frac{26}{25}fmg \tag{19}$$

where F_{fl} and F_{fr} represent the rolling resistance of the left and right wheels respectively, while f_l and f_r represent the rolling resistance coefficients of the left and right wheels respectively.

The rolling obstruction force finally acts on the forward motion of the robot, mapping it to the world coordinate system as

$$E(\xi_I)F_f\ ,E(\xi_I)^T=[cos\,\theta \quad sin\,\theta \quad 0\,] \tag{20}$$

The robot consists of two differential driving wheels as the actuator of the control system, and the left and right driving wheels form a resultant force in the form of differential speed, namely the robot centroid driving force F_c.The robot controls the steering force through the difference in torque at the wheel edges of the left and right wheels, and the expression is as follows

$$\begin{cases} F_c = T_r+T_l = \frac{\tau_r+\tau_l}{r} \\ F_\theta = \frac{(\tau_r-\tau_l)L}{2r} \end{cases} \tag{21}$$

ISSN: 2414-1895 DOI: 10.6919/ICJE.202510_11(10).0017

where T_l, T_r represents the driving torque of the left and right wheels, and τ_l, τ_r represents the torque of the left and right motors, and L represents the distance between the left and right wheels

In the global coordinate system, the driving force of the two wheels of the robot is decomposed into the X axis, Y axis and the rotation direction around the Z axis of the global coordinate system, which are expressed as follows

$$\boldsymbol{F_w}=\begin{bmatrix} F_x \\ F_y \\ F_\theta \end{bmatrix}=\boldsymbol{B}\tau=\begin{bmatrix} \frac{\cos\theta}{r} & \frac{\cos\theta}{r} \\ \frac{\sin\theta}{r} & \frac{\sin\theta}{r} \\ \frac{L}{2r} & -\frac{L}{2r} \end{bmatrix}\begin{bmatrix} \tau_r \\ \tau_l \end{bmatrix} \tag{22}$$

Where $\boldsymbol{B}$ is the driving force transformation matrix, $\boldsymbol{\tau}$ represents the torque matrix of the drive motor.

The nonholonomic constraint equations of robot without lateral motion are listed as follows

$$f_1=\dot{x}\sin\theta-\dot{y}\cos\theta=0 \tag{23}$$

where $\dot{x}$ represents the speed in the X-axis direction of the robot's world coordinate system, $\dot{y}$ represents the speed in the Y-axis direction of the robot's world coordinate system, and θ represents the heading angle of the robot's world coordinate system.

The system generalized coordinate of the medical transport nursing robot considering the sitting posture of the human body is selected as $\boldsymbol{q}=[x \quad y \quad \theta \quad \varphi_x \quad \varphi_y]^T$, and the position of the robot on the X axis and Y axis of the global coordinate system and the heading Angle between the forward direction and the X axis are selected in turn. The derivative of the generalized coordinate generalized velocity is $\dot{\boldsymbol{q}}=[\dot{x} \quad \dot{y} \quad \dot{\theta} \quad \dot{\varphi}_x \quad \dot{\varphi}_y]^T$, and the constraint term matrix can be obtained by calculating the partial derivative of q_i for the constraint equation

$$\boldsymbol{A}(\boldsymbol{q})^T=\frac{\partial f_i}{\partial \boldsymbol{q}_i}=[\sin\theta \quad -\cos\theta \quad 0 \quad 0 \quad 0] \tag{24}$$

where $\boldsymbol{A}(q)^T$ obtained in this way makes the matrix equation $\boldsymbol{A}(\boldsymbol{q})^T\dot{\boldsymbol{q}}=0$, satisfy the nonholonomic constraints of the robot.

The transformation matrix $\boldsymbol{S}$ of robot forward kinematics equation sub (7) in generalized coordinates is extended to the generalized form, and can be obtained

$$\boldsymbol{S}^T(\boldsymbol{q})=\begin{bmatrix} \frac{r\cos\theta}{2} & \frac{r\sin\theta}{2} & \frac{r}{L} & 0 & 0 \\ \frac{r\cos\theta}{2} & \frac{r\sin\theta}{2} & -\frac{r}{L} & 0 & 0 \end{bmatrix}, \boldsymbol{S}^T(\boldsymbol{q})\boldsymbol{A}(\boldsymbol{q})=0 \tag{25}$$

where $\boldsymbol{S}$ represents the forward kinematics transformation matrix.

The Lagrangian method with dissipation function is used to construct the dynamic equation of the robot

$$\frac{d}{dt}\left(\frac{\partial \mathrm{L}}{\partial \dot{\boldsymbol{q}}_i}\right)-\frac{\partial \mathrm{L}}{\partial \boldsymbol{q}_i}+\frac{\partial \boldsymbol{D}}{\partial \boldsymbol{q}_j}=\boldsymbol{B}(\boldsymbol{q})\boldsymbol{\tau}+\boldsymbol{A}(\boldsymbol{q})\lambda-\boldsymbol{E}(q)F_f$$

$$\boldsymbol{B}^{\mathrm{T}}(\boldsymbol{q})=\begin{bmatrix} \frac{cos\,\theta}{r} & \frac{sin\,\theta}{r} & \frac{L}{2r} & 0 & 0 \\ \frac{cos\,\theta}{r} & \frac{sin\,\theta}{r} & -\frac{L}{2r} & 0 & 0 \end{bmatrix} \tag{26}$$

$$\boldsymbol{P}^{T}(\boldsymbol{q})=\begin{bmatrix} \frac{r\,cos\,\theta}{2} & \frac{r\,sin\,\theta}{2} & \frac{r}{L} & 0 & 0 \\ \frac{r\,cos\,\theta}{2} & \frac{r\,sin\,\theta}{2} & -\frac{r}{L} & 0 & 0 \end{bmatrix}$$

Where $\boldsymbol{q}_i$ is the generalized vector, $\boldsymbol{B}(\boldsymbol{q})$ is the driving force term matrix, $\boldsymbol{A}(\boldsymbol{q})$ is the binding force term matrix, $\boldsymbol{P}^T(\boldsymbol{q})$ is the driving angular velocity transformation matrix.

According to the planar motion characteristics of the rigid body system, that is, the potential energy of the robot system is zero, and only the potential energy of the human body in the sitting posture is considered, the Lagrangian function $L=T_c+T_m-V_m$ of the system is substituted into equations (26) , and the Lagrangian function L equation is written

$$L=\frac{1}{2}m\left(\dot{x}^2+\dot{y}^2\right)+\frac{1}{2}I_z\dot{\theta}^2+\frac{1}{2}I_0\left(\dot{\varphi}_r^2+\dot{\varphi}_l^2\right)+T_m-V_m \tag{27}$$

where m represents the mass of the robot, $\dot{x}$ and $\dot{y}$ are the velocities of the robot's x and y axes in the global coordinate system, I_z is the moment of inertia of the robot, I_0 is the moment of inertia of the driving wheels, $\dot{\varphi}_l$ and $\dot{\varphi}_r$ are the angular velocities of the left and right driving wheels respectively, T_m is the kinetic energy of the human sitting posture, and V_m is the potential energy of the human sitting posture.

Substitute equations (6) and (27) into the Lagrangian equation and formula together

$$\boldsymbol{M}(\boldsymbol{q})\ddot{\boldsymbol{q}}+\boldsymbol{V}(\boldsymbol{q},\dot{\boldsymbol{q}})\dot{\boldsymbol{q}}+\boldsymbol{E}(\boldsymbol{q})F_f+\boldsymbol{G}(\boldsymbol{q})+\tau_d=\boldsymbol{B}(\boldsymbol{q})\tau+\boldsymbol{A}(\boldsymbol{q})\lambda \tag{28}$$

Where $\boldsymbol{M}(\boldsymbol{q})$ is a symmetric and positive definite generalized inertia matrix, $\boldsymbol{V}(\boldsymbol{q},\dot{\boldsymbol{q}})$ is the centriatic and Cauchy force matrix, F_f is the rolling obstacle force, $\boldsymbol{M}_T$ is the steering sliding friction torque, $\boldsymbol{G}(\boldsymbol{q})$ is the gravity matrix, τ_d is the external disturbance.

This is the dynamic model of the variable load medical transport nursing robot studied in this paper. According to the above matrix, there is a close coupling relationship between the pitch Angle velocity of the sitting human body and the robot motion, and the rocking of the human body will significantly affect the robot motion. The control system should be designed considering the disturbance caused by the pitch Angle of the human body on the robot.

3. Model Building for Sitting Human Mass Estimation and Swaying Recognition

3.1 Longitudinal Dynamics Model of the Robot

In the design of trajectory tracking controller for most nonholonomic mobile robot, generally based on the kinematic equation, the velocity control quantity $u(t)$ is obtained, so that the mobile robot can track the desired trajectory under the action of $u(t)$. Considering the strong nonlinear disturbances such as variable load and unknown disturbance during the operation of the robot, the speed tracking control system based on the kinematic model is not enough to meet the operation needs of the medical transport nursing robot. Therefore, the speed tracking control based on the dynamic model is added, and the speed control quantity $u(t)$ is introduced into the torque control quantity $\tau(t)$. So that the robot can sense the torque changes of human body disturbance in sitting posture.

Based on the Lagrange multiplier method modeling of the dissipation function, the dynamic equation considering the mass change and swish of the sitting human body can be expressed as

$$m_{\mathrm{h}}\mathrm{h}\dot{v}+\left(m_{\mathrm{h}}\mathrm{h}^2+m_{\mathrm{h}}\mathrm{h}^2\dot{\varphi}_y^2+I_{\mathrm{h}}\right)\ddot{\varphi}_y+2m_{\mathrm{h}}\mathrm{h}^2\varphi_y\dot{\varphi}_y^2-m_{\mathrm{h}}\varphi_y\left(\mathrm{h}^2\dot{\theta}^2+\mathrm{h}^2\dot{\varphi}_y{}^2\right)+m_{\mathrm{h}}g\mathrm{h}\,sin\,\varphi_y-k_y\varphi_y-c_y\dot{\varphi}_y=0 \tag{29}$$

where m_{h} represents the human sitting posture mass, $\dot{v}$ represents the speed of a person's sitting posture, h represents the height of the human upper body, φ_y represents the human sitting posture pitch angle, $\dot{\varphi}_y$ represents the human sitting posture pitch angle velocity, and k_y and c_y respectively represent the spring coefficient and damping coefficient of the human sitting posture lateral sway.

Considering the actual sampling frequency and speed command as constant, the above equations are simplified to obtain the shaking disturbance force of the human body as follows

$$F_{\varphi}=-m_{\mathrm{h}}\mathrm{h}\dot{v}=\left(m_{\mathrm{h}}\mathrm{h}^2+m_{\mathrm{h}}\mathrm{h}^2\dot{\varphi}_y^2+I_{\mathrm{h}}\right)\ddot{\varphi}_y+m_{\mathrm{h}}\mathrm{h}^2\varphi_y\dot{\varphi}_y^2+m_{\mathrm{h}}g\mathrm{h}\,sin\,\varphi_y-k_y\varphi_y-c_y\dot{\varphi}_y \tag{30}$$

where F_{φ} represents the human body's shaking disturbance force.

Considering that the actual operation site of the robot is flat and the running speed is low, the ground slope and wind resistance are set to 0, the ground friction coefficient f is measured by the engineering test, and the longitudinal dynamic model of the robot can be expressed as

$$\frac{(\tau_r+\tau_l)N}{r}=F_f+F_a+F_{\varphi} \tag{31}$$

where τ_{r} is the right wheel drive torque, τ_l is the left wheel drive torque, N is the drive transmission efficiency, r is the radius of the drive wheel, $F_f=f(m+m_h)g$ is the rolling resistance of the overall robot mass, $F_a=(m+m_h)\delta\frac{dv}{dt}$ is the acceleration resistance of the overall robot mass, δ is the rotation mass conversion coefficient, and other parameters have been mentioned above.

3.2 Structure of the Compensation Algorithm for Human Mass and Sway Estimation in Sitting Posture

During the driving process, the robot's own mass can be regarded as a constant parameter. At the beginning of the operation, the driving torque is large, and the error of estimating the mass of the whole vehicle using the data at this stage is small. Therefore, the overall mass of the robot can be estimated accurately within the first few seconds of the robot running. It can be used for speed tracking control of robots. The sitting body mass is also used as an input parameter of the body sway disturbance estimator to compute and compensate the body sway pitch Angle in real time.

ISSN: 2414-1895 DOI: 10.6919/ICJE.202510_11(10).0017

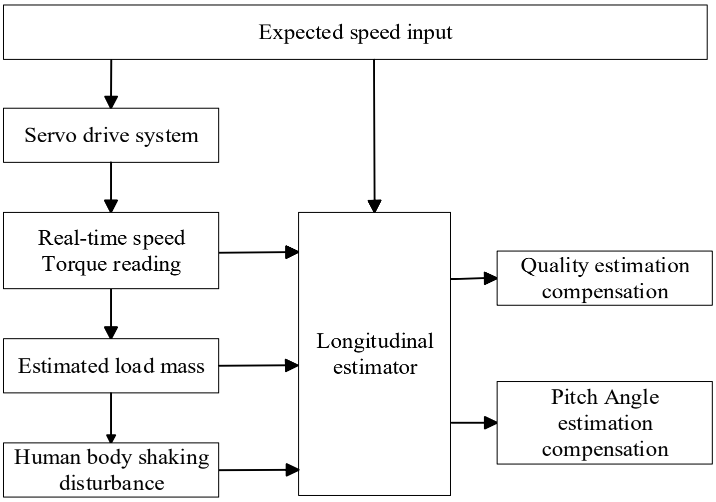

Figure 6. Estimation algorithm structure diagram

4. Algorithm for Estimating Human Body Mass and Posture-Based on Sit-Down Position

4.1 Improved FFRLS for Seated Human Mass Estimation

recursive least squares (RLS) method updates and corrects the estimated value of old data in real time by continuously collecting the latest data, so as to improve the real-time accuracy. However, with the continuous acquisition of data, the amount of data accumulates, and the influence of old data on new data increases, which reduces the effectiveness of newly acquired data and causes the problem of "data saturation" [15]. Forgetting factor is often used to adjust the weight of newly acquired data to solve this problem. However, in FFRLS, the forgetting factor is usually set as a fixed constant value, which cannot effectively meet the real-time requirements such as speed and accuracy of the system when dealing with dynamic systems with varying load. In addition, the forgetting factor has a significant impact on the convergence and stability of the algorithm. In order to solve this problem, this paper introduces the adaptive forgetting factor of threshold switching into the traditional RLS algorithm to form the threshold adaptive recursive least squares (TAFFRLS). Through the error threshold as the judgment bound, the system dynamically adjusts the value, so that the algorithm can more effectively balance the weight of the old and new data, thereby improving the speed and accuracy of parameter identification. The design idea of the adaptive forgetting factor is to dynamically adjust the size of the forgetting factor according to the absolute difference between the output value of the current theoretical model and the actual model. When the robot just starts, the driving torque is the largest and the influence of sitting body shaking on the motor torque is the smallest, so it is a better choice to estimate at this time. In the starting stage, the influence of sitting body shaking is ignored, and it is transformed into a least square problem.

$$\frac{\tau_c N}{r}=(m+m_h)(\frac{dv}{dt}+fg)\ ,\ \boldsymbol{E}_F=\frac{\tau N}{r}\ ,\ \boldsymbol{E}_a=\delta\frac{dv}{dt}+fg \tag{32}$$

where E_F is the system output, E_a is the observable data vector, m is the known mass of the robot body, and $\mathrm{m_h}$ is the predicted mass of the sitting human body.

The estimation error at time k is given by

$$\varepsilon(k)=\boldsymbol{E}_F(k)\text{-}\boldsymbol{E}_a(k)m_h(k\text{-}1) \tag{33}$$

where $E_F(k)$ represents the system output at time k, $E_a(k)$ represents the observable data vector at time k, and $m_h(k\text{-}1)$ represents the mass of the robot at time k-1.

The proposed adaptive forgetting factor function for threshold switching at time k is as follows

$$\lambda(k)=\begin{cases}\lambda_{min}, & |\varepsilon(k)|>\varepsilon_{max}\\ \lambda_{max}, & |\varepsilon(k)|<\varepsilon_{min}\\ \lambda_{min}+(\lambda_{max}-\lambda_{min})\dfrac{\varepsilon_{max}-|\varepsilon(k)|}{\varepsilon_{max}-\varepsilon_{min}}, & otherwise\end{cases} \tag{34}$$

where $\lambda_{min}\in(0,1)$ is the fast tracking mode and $\lambda_{max}\in(\lambda_{min},1]$, is the steady state mode. Considering that the piecewise function may cause a step jump, the adaptive forgetting factor function is smoothed based on threshold switching

$$\begin{cases}\lambda(k)=\lambda_{min}+(\lambda_{max}-\lambda_{min})e^{\beta}\\ \beta=-\alpha\, max(0,|\varepsilon(k)|-\varepsilon_{min})\end{cases} \tag{35}$$

where $\alpha>0$ is the error sensitivity coefficient, and the larger is α, the more drastic is the response of the forgetting factor to the error.

The estimated masses at time k-1 and k are defined as $m(k-1)$ and $m(k)$, the output of the system at time k is (k), the observable data vector is (k), and the estimation model is as follows

$$\begin{cases}m_h(k)=m_h(k-1)+\boldsymbol{K}(k)\varepsilon(k),\\ \boldsymbol{K}(k)=\dfrac{\boldsymbol{H}(k-1)\boldsymbol{E}_a(k)}{\lambda+\boldsymbol{E}_a^T(k)H(k-1)\boldsymbol{E}_a(k)},\\ \boldsymbol{H}(k)=\dfrac{1}{\lambda}[I-\boldsymbol{K}(k)\boldsymbol{E}_a(k)]\boldsymbol{H}(k-1).\end{cases} \tag{36}$$

where λ is the forgetting factor and $m_h(k)$ is the vehicle quality at each sampling time; $\boldsymbol{K}(k)$ is the least-squares gain; $\boldsymbol{I}$ is the identity matrix. $\boldsymbol{H}(k)$ is the covariance matrix, and the error covariance is carried out for updating.

The initial value of the algorithm is

$$\begin{cases}\boldsymbol{H}(0)=\left[\boldsymbol{E}_a^T(0)\boldsymbol{E}_a(0)\right]^{-1},\\ m_h(0)=\boldsymbol{H}(0)\boldsymbol{E}_a^T(0)\boldsymbol{E}_F(0).\end{cases} \tag{37}$$

where $\boldsymbol{H}(0)$,$m_h(0)$,$\boldsymbol{E}_a(0)$, and $\boldsymbol{E}_F(0)$ are their initial values.

When the robot starts, the velocity starts to change, and subsequently the estimation of the body mass in the sitting posture is carried out according to the above recursive formula.

4.2 Establishment of Sloshing Disturbance Estimation Model for Sitting Human Body

Combined with the analysis of human body dynamics, the expression of rocking disturbance of sitting human body can be derived, and its magnitude is related to the body's upper body mass, pendulum length, pitch Angle acceleration and damping coefficient. In order to realize the real-time estimation of the disturbance τ_d, it is necessary to take the human pitch Angle φ_y and its change rate $\dot{\varphi}_y$ as the observation state variables, collect the robot speed, acceleration, driving force and other information through the robot drive system in real time, and use the Unscented Kalman Filter (UKF) algorithm to estimate and predict the human pitch Angle and its change rate. Combined with the dynamic model

ISSN: 2414-1895 DOI: 10.6919/ICJE.202510_11(10).0017

of the robot considering the swish of the sitting human body, the state equation and the observation equation are constructed. And the human body sloshing disturbance τ_d is estimated and compensated.

The state space equation of the system is established, and the robot velocity and the pitch Angle of the sitting human body are selected as the system state vector $\boldsymbol{x}$=[v φ_y]^T. The differential equation of the system is given by

$$\begin{cases} \frac{dv}{dt}=\frac{\tau N}{r\delta(m+m_{\mathrm{h}})}-\frac{gf}{\delta}-\frac{F_\varphi}{\delta(m+m_{\mathrm{h}})} \\ \frac{d\varphi_y}{dt}=0 \end{cases} \tag{38}$$

where v represents the robot's speed, τ is the motor torque, N represents the driving transmission efficiency, g represents the gravitational acceleration, f represents the rolling resistance coefficient, F_φ represents the human disturbance, m and m_h represent the robot's mass and the human sitting mass, and δ represents the acceleration coefficient.

The discrete state space equation of the system is given by

$$\begin{cases} v_k=v_{k\text{-}1}+\Delta t\left(\frac{\tau N}{r\delta(n+m_h)}-\frac{gf}{\delta}-\frac{F_\varphi}{\delta(n+m_h)}\right) \\ \varphi_{y_k}=\varphi_{y_{k\text{-}1}} \end{cases} \tag{39}$$

Since the system quality parameters vary, the system equation cannot fully reflect the real physical process, and there are sensor errors in the observation, independent white Gaussian noise with zero mean should be introduced as the process noise and observation noise, which are represented by vector $\boldsymbol{W}$(k) and $\boldsymbol{V}$(k) respectively, and their covariance matrices are $\boldsymbol{Q}$ and $\boldsymbol{R}$ respectively. The following relationship can be obtained

$$\begin{gathered} E[\boldsymbol{W}(k)]=0 \\ E[\boldsymbol{V}(k)]=0 \\ E[\boldsymbol{W}(k)\boldsymbol{W}^T(k)]=\boldsymbol{Q} \\ E[\boldsymbol{V}(k)\boldsymbol{V}^T(k)]=\boldsymbol{R} \\ E[\boldsymbol{W}(k)\boldsymbol{V}^T(k)]=0 \end{gathered} \tag{40}$$

The state equation of the system under the influence of random noise can be derived as

$$\begin{bmatrix} v_k \\ \varphi_{y_k} \end{bmatrix}=\begin{bmatrix} v_{k\text{-}1}+\Delta t\left(\frac{\tau N}{r\delta(m+m_h)}-\frac{gf}{\delta}-\frac{F_\varphi}{\delta(m+m_h)}\right) \\ \varphi_{y_{k\text{-}1}} \end{bmatrix}+\boldsymbol{W}(k) \tag{41}$$

where v_k represents the robot's speed at time k, φ_{y_k} represents the human body's sitting pitch angle at time k, Δt represents the system sampling time interval, and $\boldsymbol{W}(k)$ represents the process noise at time k.

The observation equation of the system is given by

$$\boldsymbol{Y}(k)=[1 \quad 0]\begin{bmatrix} v_k \\ \varphi_{y_k} \end{bmatrix}+\boldsymbol{V}(k) \tag{42}$$

where $\boldsymbol{V}(k)$ represents measurement noise at time k.

The state space equation of the system is obtained as

$$\begin{cases} \boldsymbol{X}(k)=f(\boldsymbol{X}(k\text{-}1))+\boldsymbol{W}(k\text{-}1) \\ \boldsymbol{Y}(k)=\boldsymbol{HX}(k)+\boldsymbol{V}(k) \end{cases} \tag{43}$$

where $\boldsymbol{H}$ represents the covariance matrix, and $f(\boldsymbol{X}(k\text{-}1))$ represents the state variable for the time prediction.

It is introduced into the UKF calculation step.

1)Weight value calculation. For an n-dimensional state variable, the weight values of $2n+1$ mean and covariance are calculated as

$$\begin{cases} W_m^{(0)}=\dfrac{\lambda}{n+\lambda}, \\ W_c^{(0)}=\dfrac{\lambda}{n+\lambda}+1\text{-}\alpha^2+\beta, \\ W_m^{(i)}=W_c^{(i)}=\dfrac{1}{2(n+\lambda)}, \quad i=1,\cdots,2n \end{cases} \tag{44}$$

where $\boldsymbol{W}_m$ and $\boldsymbol{W}_c$ are the weight values of the mean and covariance, respectively; λ, α, β are Kalman filter parameters.

2)Sigma point sampling. Calculate $2n+1$ sample points from the mean and covariance

$$X_{k|k\text{-}1}^{(i)} \begin{cases} \hat{x}_{k|k\text{-}1}, & i=0; \\ \hat{x}_{k|k\text{-}1}+\left(\sqrt{(n+\lambda)P_{k|k\text{-}1}}\right)_i, & i=1,\cdots,n; \\ \hat{x}_{k|k\text{-}1}\text{-}\left(\sqrt{(n+\lambda)P_{k|k\text{-}1}}\right)_{i\text{-}n}, & i=n+1,\cdots,2n. \end{cases} \tag{45}$$

where $\hat{\boldsymbol{x}}_{k|k-1}$ and $\boldsymbol{P}_{k|k-1}$ are the state variables and the state estimation error covariance matrix at time k-1, respectively. $\boldsymbol{X}_{k|k-1}$ is the Sigma point.

3) State prediction. Through the state transition function, measurement function and weight value, the state variable, the state estimation error covariance matrix and the prior value of the measurement variable are calculated according to the formula.

$$\begin{cases} \boldsymbol{X}_{k|k-1}^{(i)}=f\left(\boldsymbol{X}_{k-1|k-1}^{(i)},\boldsymbol{u}_{k-1}\right) \\ \hat{\boldsymbol{x}}_{k|k-1}=\sum_{i=0}^{2n}\boldsymbol{W}_m^{(i)}\boldsymbol{X}_{k|k-1}^{(i)} \\ \boldsymbol{P}_{k|k-1}=\sum_{i=0}^{2n}\boldsymbol{W}_c^{(i)}\left(\hat{\boldsymbol{x}}_{k|k-1}-\boldsymbol{X}_{k|k-1}^{(i)}\right)\left(\hat{\boldsymbol{x}}_{k|k-1}-\boldsymbol{X}_{k|k-1}^{(i)}\right)^T+\boldsymbol{Q}_{k-1} \\ \boldsymbol{Z}_{k|k-1}^{(i)}=\mathrm{h}\left(\boldsymbol{X}_{k|k-1}^{(i)},\boldsymbol{u}_k\right) \\ \hat{\boldsymbol{z}}_{k|k-1}=\sum_{i=0}^{2n}\boldsymbol{W}_m^{(i)}\boldsymbol{Z}_{k|k-1}^{(i)} \end{cases} \tag{46}$$

where $\boldsymbol{X}_{\mathrm{k|k-1}}$ and $\boldsymbol{Z}_{\mathrm{k|k-1}}$ are the prior Sigma points after state transition and measurement, respectively. $\hat{\boldsymbol{x}}_{\mathrm{k|k-1}}$, $\boldsymbol{P}_{\mathrm{k|k-1}}$, and $\hat{\boldsymbol{z}}_{\mathrm{k|k-1}}$ are the prior state variables, the prior state estimation error covariance matrix, and the prior measurement variables, respectively.

4)Status updates. The gain matrix is calculated, and the state variables and the state estimation error covariance matrix are updated to finally obtain the estimated value.

$$\begin{cases} \boldsymbol{P}_{zz,k|k-1}=\sum_{i=0}^{2n}W_c^{(i)}\left(\hat{z}_{k|k-1}-Z_{k|k-1}^{(i)}\right)\left(\hat{z}_{k|k-1}-Z_{k|k-1}^{(i)}\right)^T+R_{k-1} \\ \boldsymbol{P}_{xz,k|k-1}=\sum_{i=0}^{2n}W_c^{(i)}\left(\hat{x}_{k|k-1}-X_{k|k-1}^{(i)}\right)\left(\hat{z}_{k|k-1}-Z_{k|k-1}^{(i)}\right)^T \\ \boldsymbol{K}_k=\boldsymbol{P}_{xz,k|k-1}P_{zz,k|k-1}^{-1} \\ \hat{\boldsymbol{x}}_{k|k}=\hat{x}_{k|k-1}+\boldsymbol{K}_{\boldsymbol{k}}\left(z_k-\hat{z}_{k|k-1}\right) \\ \boldsymbol{P}_{k|k}=P_{k|k-1}-\boldsymbol{K}_kP_{zz,k|k-1}K_k^T \end{cases} \tag{47}$$

where $\boldsymbol{P}_{\mathrm{zz,k|k-1}}$ and $\boldsymbol{P}_{\mathrm{xz,k|k-1}}$ are the observed covariance matrix and the cross-correlation covariance matrix of the estimation error, respectively. $\boldsymbol{K}_{\mathrm{k}}$ is Kalman gain matrix; $\hat{\boldsymbol{x}}_{\mathrm{k|k}}$ and $\boldsymbol{P}_{\mathrm{k|k}}$ are the posterior state variables and the state estimation error covariance matrix, respectively.

The above is the specific process of the algorithm, which uses Sigma points to calculate the continuous prediction mean and covariance, and inputs the results into the Kalman framework to generate the information matrix and the cross-covariance matrix. Finally, the Kalman gain is calculated and the system state is updated. The proposed adaptive process noise state estimation enables the system to predict the human sitting posture quality faster, which is added to the UKF to further predict the human swaying pitch Angle.

5. Simulation Analysis

By building an algorithm model, the mass estimation algorithm and the human body sway estimation algorithm are tested. The physical parameters of the medical transfer nursing robot used in the test are shown in Table 2, and the data are based on the actual measurement results of the medical transfer nursing robot.

 Volume 11 Issue 10, 2025
DOI: 10.6919/ICJE.202510_11(10).0017

Table 2. Physical parameters of medical transport nursing robot

Physical parameters	Numerical value
Robot mass $m(kg)$	160
Drive track $L(m)$	0.7
Wheel rolling radius $r(m)$	0.0825
Rated torque of the drive wheel $T(Nm)$	21
Rated driving force of differential wheel $F_{drive}(N)$	533
The moment of inertia of the driving wheel $I_w(kg\ m^2)$	0.0004
Drive wheel mass $m_0(kg)$	1.7
The moment of inertia of the robot around the Z-axis $I_c(kg\ m^2)$	20

The driving condition is set as 0-5km /h on the horizontal road, and the starting threshold of the mass estimation algorithm is set as 0.5km/h. The human body mass estimation in sitting posture and human pitch Angle estimation under the robot torque control are shown in Figures. 7 and 8.

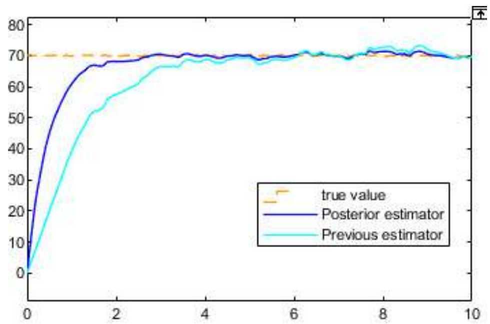

Figure 7. Human body mass estimation in sitting posture

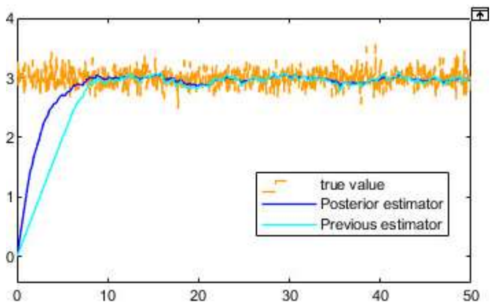

Figure 8. Human pitch Angle estimation in sitting posture

According to the analysis of the simulation results, in Figure 7, by comparing the estimation algorithm before and after improvement, it can be seen that the improved method proposed in this paper reaches a stable state in the second second, and can estimate the human mass in the sitting posture faster. In Figure 8, by comparing the estimation algorithm before and after improvement, it can be seen that the improved method proposed in this paper quickly tracks the estimated value of the sitting human body pitch Angle to the initial sitting human body pitch Angle at about 5 to 6 seconds, which can track the pitch Angle faster.

6. Conclusion

In this paper, aiming at the problem of sitting human body mass change and shaking interference faced by medical transport nursing robot in the transport process, the global dynamic model of medical transport nursing robot is established based on the dissipation function Lagrange equation. The improved adaptive recursive least squares method and adaptive Unscuted Kalman filter were used to estimate the unknown and changing sitting posture human body mass parameters and the unmeasurable shaking pitch Angle respectively. Through simulation verification, the tracking rapidness and accuracy of the robot in human sitting posture mass and pitch Angle change were effectively improved.

References

[1] D.J. Wang, Y.D. Zhu, Y. Chen, et al. Optimal Design and Ride Comfort of Logistics AGV Robot Suspension System (Manufacturing Automation, China 2023), p.139-143. (In Chinese)

[2] H.M. Song, Y.F. Yao, C. Lin, et al. Research Progress and Development Trends of Transfer Nursing Robots (Machinery Design & Manufacture, China 2020), p.162-165+169. (In Chinese)

[3] H. Guo, D. Cao, H. Chen, et al. Vehicle dynamic state estimation: state of the art schemes and perspectives (IEEE/CAA Journal of Automatica Sinica, 2018), p.418-431.

[4] X. Li, J. Ma, X. Zhao, et al. Intelligent Two-Step Estimation Approach for Vehicle Mass and Road Grade (IEEE Access, 2020), p.218853-218862.

[5] M. Hu, W. Gao, Y. Zeng, et al. Vehicle Mass and Road Grade Estimation Based on Adaptive Forgetting Factor RLS and EKF Algorithm (Proc. 5th Int. Conf. Power Renew. Energy, Shanghai, 2020), p.342-346.

[6] G.R. Petrovi, J. Mattila. Analytic Solutions for Wheeled Mobile Manipulator Supporting Forces (2022).

[7] B. Wang, H. Wang, L. Wu, et al. Truck Mass Estimation Method Based on the On-board Sensor (Proc. IMechE Part D: J. Automob. Eng., 2020).

[8] L. Cai, H. Wang, T. Jia, et al. Two-layer Structure Algorithm for Estimation of Commercial Vehicle Mass (Proc. IMechE Part D: J. Automob. Eng., 2020), p.378-389.

[9] T.Y. Chuang, X.D. Zhang, C.K. Chen. Estimating the Roll Angle for a Two-Wheeled Single-Track Vehicle Using a Kalman Filter (Sensors, 2022), p.8991.

[10] Z. Li, X. Cui, Z. He, et al. A Novel Method for Electric Vehicle Insulation Detection Based on the Extended Kalman Filter Algorithm (Measurement, 2024), p.114419.

[11] E. Li, W. He, H. Yu, et al. Model-Based Embedded Road Grade Estimation Using Quaternion Unscented Kalman Filter (IEEE Trans. Veh. Technol., 2022), p.3704-3714.

[12] Y. Zhang, M. Li, Y. Zhang, et al. An Enhanced Adaptive Unscented Kalman Filter for Vehicle State Estimation (IEEE Trans. Instrum. Meas., 2022), p.1-12.

[13] Z.F. Lin. Research on Dynamic Characteristics of Seated Human Body under Vertical-Lateral-Roll Vibration Excitation (Tianjin University, China 2023). (PhD Thesis).

[14] J. Hohannes, T. Stahl, A. Lauer, et al. Evaluation of Transmission Losses of Various Dedicated Hybrid Transmission (DHT) with a Lossmap-Based Simulation Model (Automotive and Engine Technology, 2019), p.29-36.

[15] M. Hu, W. Gao, Y. Zeng, et al. Vehicle Mass and Road Grade Estimation Based on Adaptive Forgetting Factor RLS and EKF Algorithm. In: Proceedings of the 5th International Conference on Power and Renewable Energy (ICPRE 2020), Shanghai, China, 2020, p. 342-346.